Electrical and Computer Engineering Faculty Research & Creative Works

Electrical and Computer Engineering

01 Jul 2019

Spatially Continuous Strain Monitoring using Distributed Fiber Optic Sensors Embedded in Carbon Fiber Composites

Sasi Jothibasu

Yang Du

Sudharshan Anandan

Gurjot S. Dhaliwal

et. al. For a complete list of authors, see https://scholarsmine.mst.edu/ele_comeng_facwork/3833

Recommended Citation

Spatially continuous strain monitoring using distributed fiber optic sensors embedded in carbon fiber composites

Sasi Jothibasu,[a] Yang Du,[a] Sudharshan Anandan,[b] Gurjot S. Dhaliwal,[b] Rex E. Gerald II,[a] Steve E. Watkins,[a] K. Chandrashekhara,[b] and Jie Huang[a,*]
[a]Missouri University of Science and Technology, Department of Electrical and Computer Engineering, Rolla, Missouri, United States
[b]Missouri University of Science and Technology, Department of Mechanical and Aerospace Engineering, Rolla, Missouri, United States

Abstract. A distributed fiber optic strain sensor based on Rayleigh backscattering, embedded in a fiber-reinforced polymer composite, has been demonstrated. The optical frequency domain reflectometry technique is used to analyze the backscattered signal. The shift in the Rayleigh backscattered spectrum is observed to be linearly related to the change in strain of the composite material. The sensor (standard single-mode fiber) is embedded between the layers of the composite laminate. A series of tensile loads is applied to the laminate using an Instron testing machine, and the corresponding strain distribution of the laminate is measured. The results show a linear response indicating a seamless integration of the optical fiber in the composite material and a good correlation with the electrical-resistance strain gauge results. The sensor is also used to evaluate the strain response of a composite-laminate-based cantilever beam. Distributed strain measurements in a composite laminate are successfully obtained using an embedded fiber optic sensor. © *2019 Society of Photo-Optical Instrumentation Engineers (SPIE)* [DOI: 10.1117/1.OE.58.7.072004]

Keywords: fiber optic sensor; strain monitoring; embedded sensing; distributed sensing; optical frequency domain reflectometry; Rayleigh backscattered spectrum.

Paper 181570SS received Nov. 2, 2018; accepted for publication Jan. 8, 2019; published online Feb. 5, 2019.

1 Introduction

Fiber optic sensors (FOSs) offer many advantages as in-situ sensors for composite structures. They are well suited to the demands of composite fabrication and application, and they can provide flexible internal measurement options without degrading the host composite structure.[1] Composite materials are extensively used in various fields, such as aerospace, automotive, wind turbine, shipping, sports, and the recreation market. These advanced materials have advantages, such as low density, high-specific strength and stiffness, good vibration damping, long fatigue life, high wear, corrosion resistance, temperature resistance, and strong tailorability.[2–5] Structural composites for these applications can be subjected to heavy loads and extreme service conditions. Unfortunately, in-place inspection of composites is difficult or expensive. Nondestructive techniques, such as ultrasonic testing, radiography, thermography, eddy current testing, etc., can be used to detect damage in a composite laminate. However, these techniques typically require expensive equipment and intensive labor.[2] Structural health monitoring (SHM) techniques can incorporate surface-mounted or embedded sensors to address the onset of damage and catastrophic failure.[6] Sensors such as strain gauges, piezoelectrics,[7] MEMs, and fiber optics[8,9] are commonly used for SHM of composite materials.[10] A disadvantage of using the strain gauges and piezoelectric sensors is that they are susceptible to electromagnetic interference (EMI).[10] Also, most of the sensors listed above are capable of sensing only localized strains or operate over limited temperature range. Optical fiber sensors have shown the capability to give reliable strain measurements[11] even for cases of high fatigue, high temperatures, and structural damage, and they can be used as field instruments.[12–14]

FOSs, when compared to other sensors, exhibit many advantages such as immunity to EMI, wide operating temperature range, compact size, low cost, light weight, and easy embedment.[10] FOSs are used to sense temperature, strain, and refractive index, either as localized sensors or as distributed sensors. Standard fiber Bragg gratings (FBGs),[15,16] Fabry–Perot fiber sensors,[17–19] interferometric FOSs,[20] fiber optic micro bend sensors, distributed sensors, and hybrid sensors[21] are some of the different types of FOSs.[10] Multiplexed sensing is achieved by combining and arranging many discrete sensors along the length of the optical fiber for multiple point strain and temperature sensing. Hybrid sensors simultaneously measure strain, temperature, and thermal strain of the composite materials by combining and arranging different sensors in a single fiber.[21] FBGs can be multiplexed, and a multiplexed FBG is known as a multipoint sensor or quasidistributed sensor.[10] However, strain build-up at potential blind spots (e.g., in between two consecutive FBGs) cannot be measured using these point sensors as they are not continuous. Distributed sensors are employed for continuous profile monitoring with the fiber itself used as a sensor based on Brillion scattering, Raman scattering (inelastic), and Rayleigh scattering (elastic).[10,22] The advantage of distributed sensing over multiplexed point sensing is that spatially continuous measurement without dark zones can be achieved.[23] Also, since no external modifications are made to the fiber, long distance sensing of temperature and strain can be measured.[23] Rayleigh backscattering is due

to random refractive index changes along the length of the optical fiber. Rayleigh scattering along an optical fiber can be modeled as a series of Bragg grating sensors located along the length of the fiber.[3] Based on Rayleigh scattering, distributed fiber optic sensing is categorized as optical time domain reflectometry (OTDR) and optical frequency domain reflectometry (OFDR).[24–27] Conventionally, Raman or Brillouin scattering–based OTDR have limited spatial resolution (∼m) due to the inherent nature of OTDR technology.[26] In comparison, Rayleigh scattering-based OFDR is capable of achieving a spatial resolution of up to cm or even sub-cm levels.

There has been significant interest in embedding FOSs in composite laminates in recent years. Many recent studies demonstrate the popularity of SHM of composites using FOS by surface bonding of the optical fibers. For example, multiplexed FBGs and distributed fiber optic sensing using OFDR were used to monitor dynamic strain and fatigue damage of a composite axial fan blade and composite step lap joint, respectively, by attaching the fiber on the top and bottom surfaces.[28,29] Hand-layup and pre-preg layup are some of the methods to embed the FOS in the intermediate layers of the composite laminate.[30] There are many techniques such as braided composites embedded with FOS, and FOS stitched carbon fiber preforms for advanced composite structures that employ the embedding of FOS within the composite structure to maintain structural integrity.[30,31] Examples are reported describing the successful embedment of polarimetric sensors,[32] fiber Bragg grating sensors,[15] photonic crystal fiber interferometric sensors,[20] and hybrid sensors[21] in composite laminates. The FOS reported in these examples are point sensors that are embedded in the intermediate layers of the composite. In the traditional surface-bonded OFDR-based distributed strain sensing technique, it is not possible to accurately reveal the internal strain profile of the composite laminates, which are critical for guiding composite material designs. OFDR-based distributed sensing using optical fibers embedded inside composite materials remains to be explored.

In this work, a distributed FOS was embedded within the layers of composite laminates to monitor the spatially continuous profile of strain using the OFDR system. This paper presents strain sensing using unmodified optical fibers and OFDR instrumentation. The sensor performance is investigated using an INSTRON tensile testing system and a cantilever beam experiment using optical fibers, which are embedded within the composite samples, unlike the surface bonding approach. A surface-bonded electrical resistance strain gages gave additional verification for the measured tensile test. The carbon fiber/epoxy composite samples were manufactured by the out-of-autoclave (OOA) technique, using six layers of IM7/Cycom 5320-1 prepreg. The OFDR system can achieve a spatial resolution of 1 cm and can measure a minimum strain of 10 $\mu\varepsilon$. The optical fiber used is a standard single-mode fiber. The OFDR technique was used to analyze the backscattered signal. The shift in the Rayleigh backscattered spectrum (RBS) is linearly related to a change in strain in the composite materials. In addition to the demonstration of the OFDR capabilities, this work shows the seamless integration of distributed sensors in composite materials and the ability to monitor fabrication quality or structural health.

2 Methodology

2.1 Composite Sample Fabrication

An optical fiber sensor embedded in a composite sample, exhibited in Fig. 1, was manufactured according to the OOA technique. A schematic of the composite sample is shown in Fig. 1(a). A laminate structure using six layers of the IM7G/Cycom5320-1 prepreg composition, which contains the embedded optical fiber sensor, is shown in Fig. 1(b). Prepreg layers were cut to a nominal size of 304.9 mm × 76.2 mm (12 in. × 3 in.) and laid on an aluminum mold. The compacted thickness of the sample was 1.5 mm (0.059 in.). For the tensile test, a standard single-mode FOS was embedded between the central (third and fourth) layers of the composite sample. For the cantilever experiment, the optical fiber was placed between the first and second layers or fifth and sixth layers of the composite. The placement of the FOS was important because, if done improperly, local distortions could result in the degradation of the structural performance.[15] Heat shrink-tubes were used at the ingress and egress points to prevent damage to the optical fiber due to high-stress concentrations [Fig. 1(a)].

The prepreg layup was cured following the manufacturer's recommended cure cycle at a vacuum pressure of 28 in. Hg. A two-step cure cycle was used to cure the composite [Fig. 1(c)]. The layup was first heated to 140°F (60°C) to maximize the mobility of the reacting groups and then cured at 265°F (129.4°C). The sample was then subjected to a free-standing postcure soak at 350°F (177°C) for 2 h. The overall manufacturing procedure was used to fabricate six-layer cross-ply and unidirectional composite samples with embedded FOSs.

Figure 1(d) shows the cross-section image of an embedded optical fiber in the unidirectional composite laminate. The clear interface between the optical fiber and the epoxy matrix is observed in the figure. The initial diameter (250 μm) of the outer cylinder in Fig. 1(d) includes the outer coating of the optical fiber. The optical fiber was compressed, which caused it to expand slightly in the horizontal direction (285 μm) making the cross-section of the optical fiber appear like an oval shape instead of a circle. The compression of the optical fiber occurred during the composite laminate manufacturing conditions because the composite material and the embedded sensor were subjected to high temperature and pressure along the stack direction (265°F and 28 in. Hg, respectively). However, the compression of the coating layer of the optical fiber does not influence the sensor behavior since the light signal is confined to the optical fiber core. Also, the continuous interface formed between the epoxy matrix material and the optical fiber results in good strain transfer between the composite material and the optical fiber. Regarding the strain sensing performance in OFDR, an embedded optical fiber is able to provide a consistent strain sensing response only if the embedding-induced fiber loss is smaller than 6 dB. This is due to the fact that both reference and measurement information are both exacted from the same embedded optical fiber sensor.

2.2 Optical Frequency Domain Reflectometry Theory and Measurement Principle

The distributed sensing approach used in the current work is based on Rayleigh backscattering. An OFDR system can be
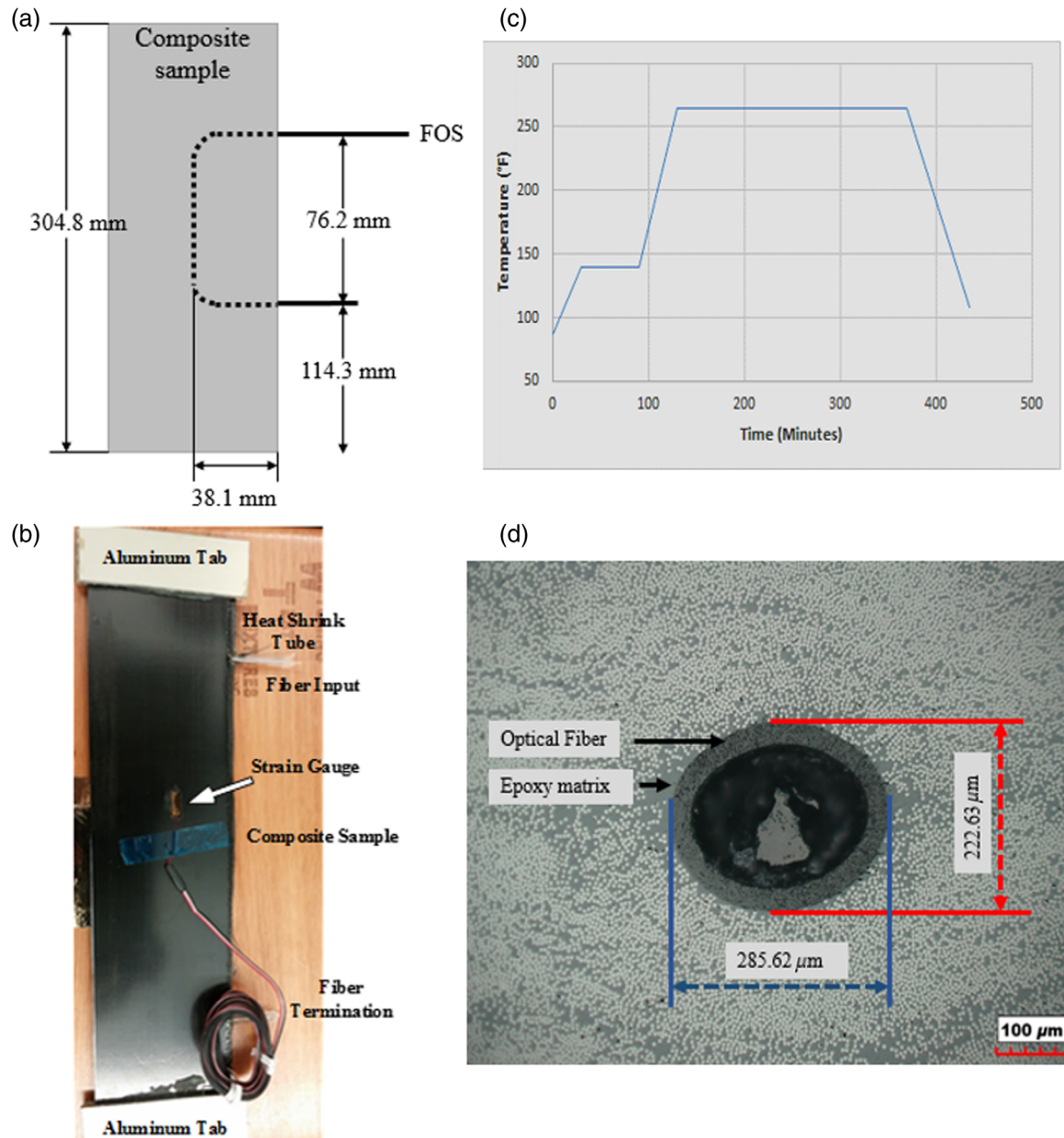
Fig. 1 Details of an embedded optical fiber sensor: (a) schematic of an optical fiber embedded in a composite sample, (b) photograph of composite sample with a reference strain gauge attached to the surface, (c) manufacturer-recommended temperature versus time cure cycle for IM7G/Cycom5320-1 prepreg system, and (d) cross-section image of the optical fiber embedded in the unidirectional composite structure.

used to sense a continuous profile of temperature and strain.[3,24,33,34] The OFDR system can achieve very high sensitivity and spatial resolution (1 $\mu\varepsilon$ and 1 cm, respectively), but there is a trade-off between measurement resolution, spatial resolution, and sampling rate for the scattering-based distributed sensing techniques.[3,24,25,33,34] The optical fiber for this work was not of the type that maintains light polarization. The required polarization control for the interferometer originates from the polarization controller used in the main interferometer.

Initially, the reference signal was recorded under conditions of no strain using a few scans by the OFDR system, and then the measured signal under strain conditions was used to analyze the RBS. The optical frequency domain signal obtained was converted into a spatial domain signal through a fast Fourier transform (FFT). A sliding window (Δx) is used for the entire range of frequencies, and each window location was converted back to the optical frequency domain. Cross correlation of the reference signal and the measured signal was done to check the spectral shift of the backscattered spectrum, which corresponds to the change in strain.

The experimental setup for displaying distributed strain measurement of the embedded fiber in a composite laminate using the OFDR technique is shown in Fig. 2.

The tunable laser source (TLS, Agilent 81680A) is used as the light source for the OFDR system. The tuning speed,
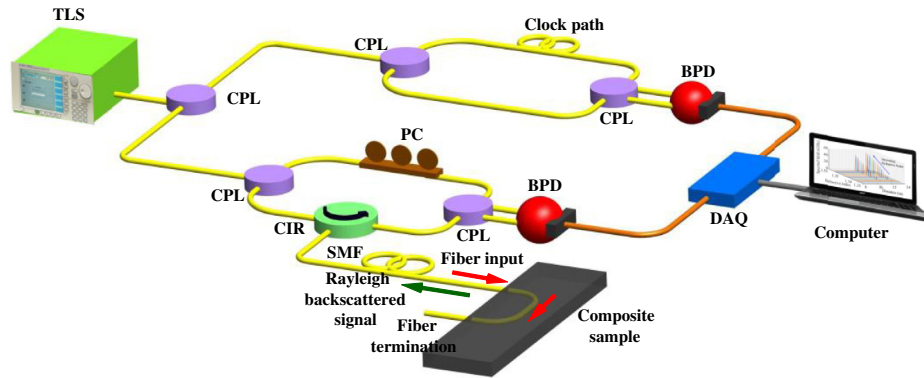
Fig. 2 Experimental setup for distributed strain measurements of the embedded optical fiber in a composite laminate. TLS, tunable laser source; CPL, coupler; CIR, circulator; SMF, single mode fiber; PC, polarization controller; BPD, balanced photodetector; and DAQ, data acquisition card.

tuning range, and starting wavelength of the TLS are 5×10^3 GHz/s (40 nm/s), 2.5×10^3 GHz (20 nm), and 1525 nm, respectively. The light from the source is split by a coupler (10/90) and takes two paths. One path is through the auxiliary interferometer (delay fiber length, 120 m), and the other path is through the main interferometer. A Mach–Zehnder auxiliary interferometer is used to provide an external clock for the data acquisition card (DAQ). It solves the nonlinear effect problem of the tunable laser, which scans the frequency range and gives the correct time base corresponding to the DAQ.[22,25] The light through the main interferometer is split and takes a reference path and a signal path by making use of a coupler (50/50). The signal path incorporates the circulator whose one arm has the fiber under test (FUT; fiber length, 10 m), which is embedded in the composite laminate. The polarization controller (Thorlabs, FPC024) is used in the reference arm to modify the polarization state of light. The backscattered light from the FUT is collected using the same coupler. The reference and the backscattered light are combined using a coupler and detected using the balanced photo detector (BPD, Thorlabs, PDB 450C). The position of the optical fiber in the composite sample (test fiber) and the instrumentation optical fiber are easily differentiated in the spatial domain signal at the splice point where the FUT is attached.
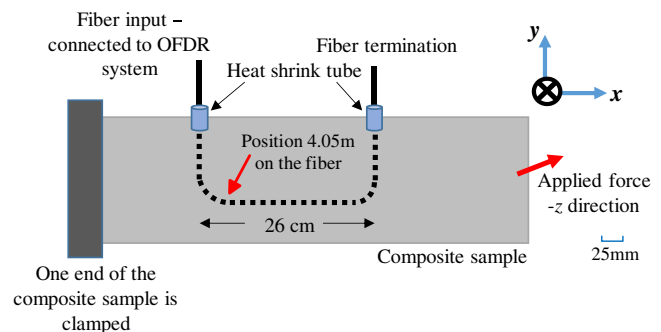
2.3 Experiments

Two types of strain tests were conducted. The first arrangement was a tensile test with the main run of the optical fiber set to measure tensile strain in a uniform sample. The second arrangement was a cantilever beam test with the optical fiber subjected to varying axial strain. For the tensile test, an electrical resistance strain gage was colocated at a central point to provide an independent measure of strain.

The composite laminate with the embedded FOS was tested for distributed strain sensing under tensile loads. Aluminum tabs 7.62 cm × 2.54 cm (3 in. × 1 in.) were attached to the ends of the composite samples using structural epoxy adhesive. Three replicates of both unidirectional and cross-ply samples were tested. The testing was done using an Instron 5985 universal testing machine, as shown in Fig. 3. The tensile testing was performed using a strain rate of 1.27 mm/min (0.05 in./min). Samples were tested up to 600 $\mu\varepsilon$, which is below the failure threshold of the composite samples. Importantly, the embedded FOS was

employed for a range of strain measurements that were well below the known upper limit (8000 microstrains) for reproducible strain measurements by optical fiber sensors.[35–38] The signals were recorded using a DAQ. Signal processing of the Rayleigh-backscattered spectra was performed to analyze and study the strain in the composite samples. A strain gauge was fixed at the center of the composite sample to compare the results with our OFDR system, which metered continuous strain values along the length of the optical fiber.
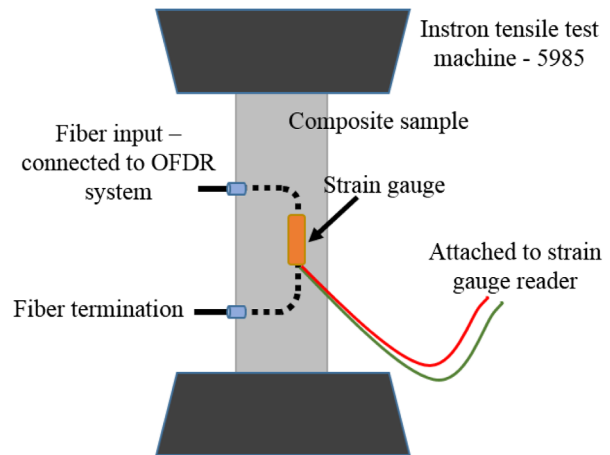
Fig. 3 Tensile testing of a composite sample using the Instron 5985 machine.

Fig. 4 Distributed strain testing of a composite sample using a cantilever experiment.
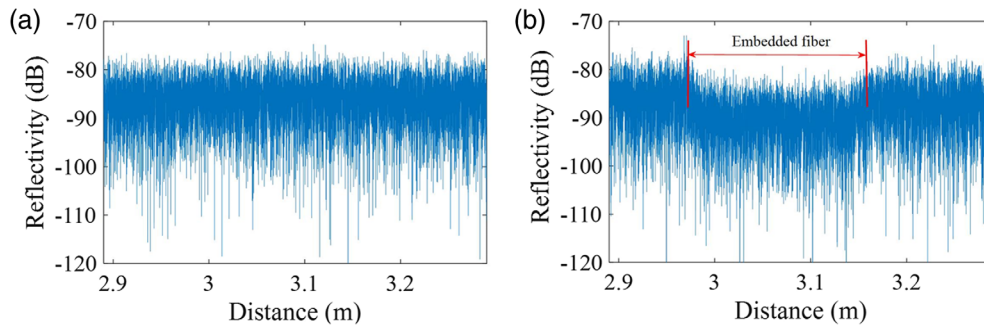
Fig. 5 Comparison of Rayleigh backscattering measurement results (a) before and (b) after the optical fiber was embedded in the composite sample.

After testing the composite samples with the Instron test machine, a cantilever beam experiment was conducted to evaluate the distributed strain sensing capability of the optical fiber embedded in a composite sample. Figure 4 shows the composite sample fixed in a cantilever beam-like structure. One end was clamped, and a force was applied on the other end of the cantilever beam in the negative z-direction. The optical fiber was embedded under the uppermost layer of the composite specimen to measure strain under cantilever-type loading. The end of the cantilever beam was displaced up to 25 mm, and the resulting strain was recorded.

3 Results and Discussion

In this section, the results of continuous strain monitoring of the composite samples under tensile loading are presented.

Prior to applying tensile loads to our samples, a comparison of the Rayleigh backscattering measurement results obtained from the optical fiber sensor before and after the fiber was embedded in the composite samples was performed. A typical result is shown in Fig. 5. Figure 5(b) reveals that an inevitable signal reduction is observed over the region of the embedded section of the optical fiber. Nevertheless, the signal losses on both sides of the input/output fiber are <4 dB, which is acceptable for our OFDR-based distributed optical fiber strain sensor. The cross-ply layup composite sample and the unidirectional composite sample correspond to samples A and B, respectively. Figures 6(a)–6(d) show the distributed sensing results from the optical fiber embedded within the composite sample with a spatial resolution of 1 cm. Loading and unloading were performed
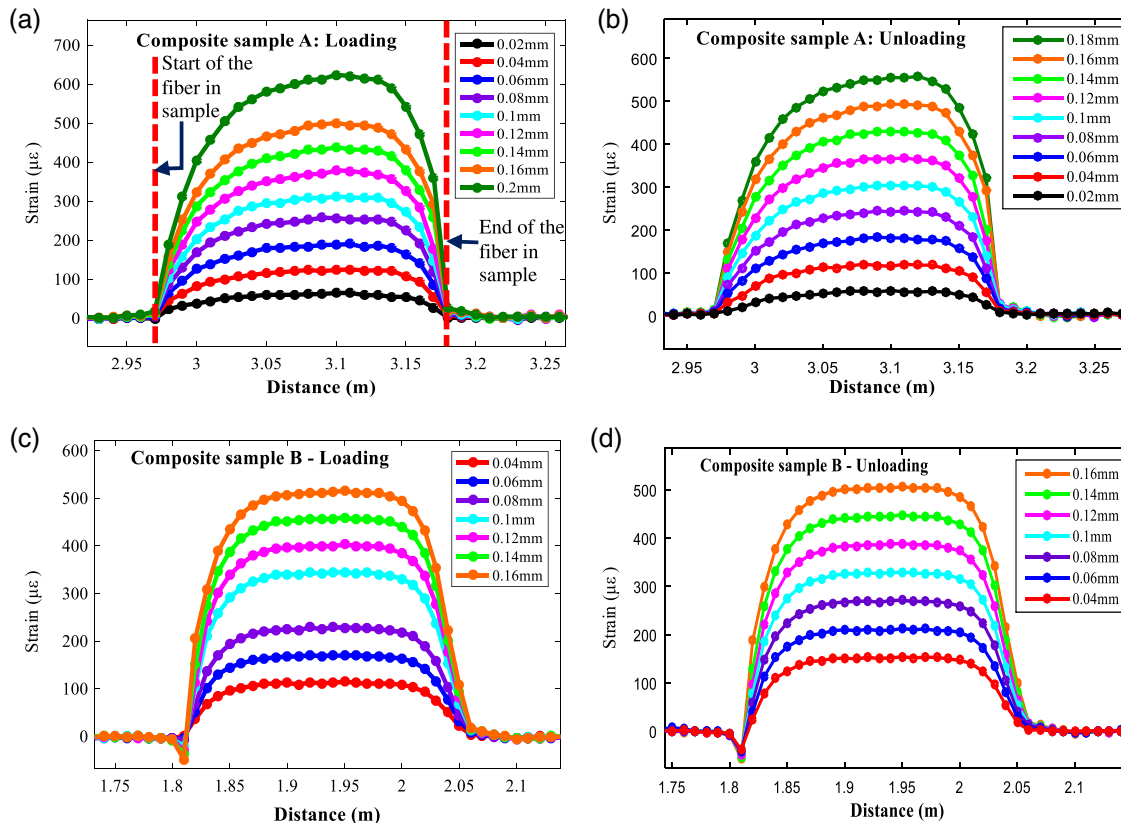
Fig. 6 Distributed strain response of the optical fiber embedded in (a) composite sample A while loading, (b) composite sample A while unloading, (c) composite sample B while loading, and (d) composite sample B while unloading.

in a stepwise manner, and strain values were monitored using the FOS. The loading and unloading curve patterns follow closely to each other, which indicate a good embedment of the optical fiber in the sample.

As shown in Fig. 6(a), the strain increases as the applied displacement increases. The maximum strain of 600 $\mu\varepsilon$ is observed when the applied maximum displacement is 0.2 mm, as shown in Fig. 6(a). Similar results are shown in Figs. 6(b)–6(d). The distributed strain drops to zero at the beginning and end of each semirectangular plot because of the shape of the optical fiber embedment in the composite sample, as shown in Fig. 3. The optical fiber measures strain in the in-plane direction only. The distributed strain values plotted for composite sample A are slightly asymmetric (not rectangular) compared to the plots for composite sample B. The observation may be due to a slight variation in the orientation of the optical fiber embedded inside the composite laminate, compared to the direction of the loading axis. This asymmetry can be avoided by the careful placement of the optical fiber using a curve-shaped geometry. The optical fiber response in other locations other than within the composite is zero, which shows the uniformity of the system (i.e., minimal crosstalk from the composite sensing region). The negative strain, ~1.8 m in composite

sample B [Figs. 6(c) and 6(d)], may be due to localized stress concentration at the edges of the composite sample.

The distributed strain values measured by the optical fiber are compared to the strain gauge output as shown in Figs. 7(a) and 7(b). A polynomial of degree one fits the experimental data well. From Figs. 7(a) and 7(b), it is found that the experiment shows good correlations between the strain gauge values and the OFDR strain values for both the loading and unloading conditions of the composite samples A and B. The R-squared values are predominantly 0.999 for all of the strain tests. The slopes of the curves while unloading for both the samples is slightly decreased by 2% when compared to the slopes of the loading tests, demonstrating that the loading and unloading curves reproducibly follow each other. The reproducibility demonstrates a faithful strain transfer between the composite laminate and the optical fiber. Figure 8 was derived from Fig. 6(a) and details the comparison between the strain gauge output and the OFDR strain values with error bars for the loading condition.

The measurements from the reference electrical resistance strain gauges were in good agreement with the FOS values. A typical comparison from the tensile tests is an FOS strain of 311 $\mu\varepsilon$ and the reference gauge strain of 271 $\mu\varepsilon$ at 0.1 mm
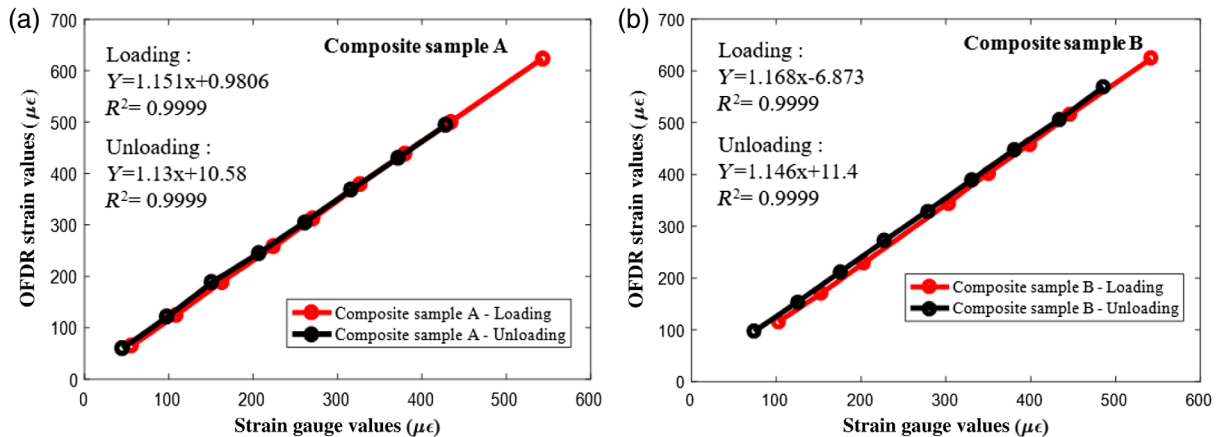

Fig. 7 Comparison of strain gauge values and maximum strain OFDR values for loading and unloading (a) composite sample A and (b) composite sample B.
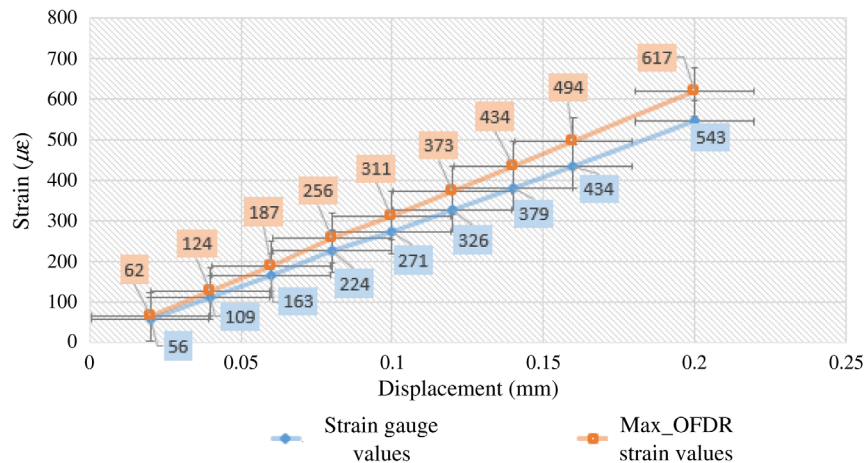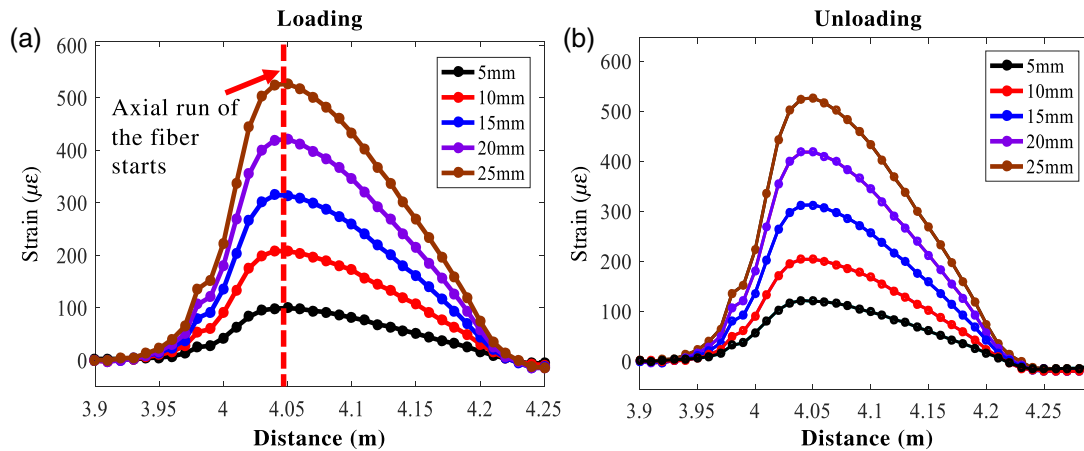

Fig. 8 Comparison of strain gauge values and maximum strain OFDR values for loading of composite sample A, including error bars derived from Fig. 6(a).

Fig. 9 Distributed strain testing of a composite laminate from a cantilever experiment. Distributed strain values using the OFDR while (a) loading and (b) unloading.

displacement, as shown in Fig. 8; the reason for the difference may be due to the embedding process and surface attachment of the FOS and some variability in the reference strain gauge, respectively.

The results from the cantilever experiment shown in Figs. 9(a) and 9(b) demonstrate a good linear sensor response. The initial increase of the strain values from 3.9 to 4.05 m is due to the curved embedding geometry of the fiber within heat shrink tubes in the laminate sample. We observed a maximum strain of ~500 $\mu\varepsilon$ at 4.05 m [Figs. 9(a) and 9(b)], which is the starting point position of the cantilever beam (see Fig. 4). As expected, the strain readings decrease along the length of the cantilever beam, away from the clamped end. The optical fiber detects the decrease in strain. The corresponding loading and the unloading strain values match each other, which demonstrate the seamless integration of the optical fiber in the composite sample with no slippage or hysteresis issues. It should be noted that the small amount of compression of the optical fiber shown in the microscope image in Fig. 1(d) did not significantly change the Rayleigh-backscattered signal, which is an advantage of the OFDR system. In our conducted OFDR strain sensing system, the strain sensitivity is 10 GHz/$\mu\varepsilon$ (80 pm/$\mu\varepsilon$) and the minimum strain that could be detected is 2.5 $\mu\varepsilon$. In our current study, the strain variation for both tensile test and cantilever beam test is around 50 $\mu\varepsilon$. Consequently, our system is able to provide sufficient sensitivity to realize the strain sensing experiments. Compared with other distributed strain sensing technologies, our established OFDR strain sensing system is capable of offering similar strain sensing sensitivity, and in addition, a very competitive spatial resolution for field applications.

4 Conclusion

The sensing of distributed strain in composite materials using OFDR has been demonstrated. A single-mode optical fiber embedded within the layers of a composite laminate was used effectively as a sensor. The shift in the Rayleigh-back-scattered signal is proportional to the change in strain within the composite material. The strain measurements by the optical fiber were validated using a tensile testing machine and a cantilever beam experiment. The results show a linear response between metered displacements and the measured strains. The results were validated using an electrical resistance strain gauge bonded to the surface of the tensile test sample. Rayleigh scattering is sensitive to both temperature changes and load-induced changes. In this investigation, the temperature was held constant during the tests.

OFDR-based distributed strain sensing with an optical fiber embedded in the intermediate layers of composites provides an effective assessment of internal strain. Applications include the characterization of strain and temperature during fabrication, quality assurance for structures, damage assessment, etc. For instance, structural health monitoring helps identify locations of stress concentrations, paths of stress propagation, and areas subjected to fatigue. Spatially disposed strain measurements data help to identify and direct the re-enforcement and repairs of distressed structural areas, avoiding catastrophic failure well in advance. The proposed techniques employed in this paper can be used to continuously monitor the health of large rigid structures with a spatial resolution of 1 cm. For laboratory testing, the resolution for strain measurements was 1 mm.

For field applications, the strain measurements by the OFDR-based methods discussed in this work will be affected by temperature. Corrections to the strain measurements data for variations in temperature can be made by employing an optic switch dividing the fiber into two parts. One part of the optical fiber that is embedded in the sample measures the temperature and strain of the FUT, and the other optical fiber should be held loose (not embedded) and thus only measures the temperature. The temperature effects measured by the loose optical fiber are subtracted from the embedded optical fiber strain measurements to determine the corrections for temperature. Some of the OFDR device challenges include the high cost of the OFDR interrogation system and the sensitivity of the OFDR system to light polarization. Future work includes the development of a low-cost OFDR interrogation system. Also, future work will examine the simultaneous measurements of strain and temperature for the FOS embedded in composite materials.

Kaur, Steve E. Watkins, K. Chandrashekhara, and Jie Huang, "Strain monitoring using distributed fiber optic sensors embedded in carbon fiber composites," Proc. SPIE 10598, Sensors and Smart Structures Technologies for Civil, Mechanical, and Aerospace Systems 2018, 105980I (27 March 2018).

References

1. A. M. Vengsarkar et al., "Low-profile fibers for embedded smart structure applications," *Proc. SPIE* **1588**, 2–13 (1991).
2. J. Cai et al., "Structural health monitoring for composite materials," in *Composites and Their Applications*, N. Hu, Ed., InTech, Rijeka, Croatia, pp. 37–60 (2012).
3. Z. Chen et al., "Ultraweak intrinsic Fabry–Perot cavity array for distributed sensing," *Opt. Lett.* **40**(3), 320–323 (2015).
4. S. Anandan et al., "Monitoring of out-of-autoclave BMI composites using fiber optic sensors," *Proc. SPIE* **8694**, 86940M (2013).
5. N. Takeda, "Summary report of the structural health-monitoring project for smart composite structure systems," *Adv. Compos. Mater.* **10**(2–3), 107–118 (2001).
6. W. B. Spillman, "Sensing and processing for smart structures," *Proc. IEEE* **84**(1), 68–77 (1996).
7. C. A. Ramos, R. de Oliveira, and A. T. Marques, "Implementation and testing of smart composite laminates with embedded piezoelectric sensors/actuators," *Mater. Sci. Forum* **587**, 645–649 (2008).
8. H.-N. Li, D.-S. Li, and G.-B. Song, "Recent applications of fiber optic sensors to health monitoring in civil engineering," *Eng. Struct.* **26**(11), 1647–1657 (2004).
9. E. Udd, "Fiber optic smart structures," *Proc. IEEE* **84**(6), 884–894 (1996).
10. M. Ramakrishnan et al., "Overview of fiber optic sensor technologies for strain/temperature sensing applications in composite materials," *Sensors* **16**(1), 99 (2016).
11. F. Akhavan, S. E. Watkins, and K. Chandrashekhara, "Measurement and analysis of impact-induced strain using extrinsic Fabry–Perot fiber optic sensors," *Smart Mater. Struct.* **7**(6), 745–751 (1998).
12. V. E. Zetterlind, S. E. Watkins, and M. W. Spoltman, "Fatigue testing of a composite propeller blade using fiber-optic strain sensors," *IEEE Sens. J.* **3**(4), 393–399 (2003).
13. A. Kaur et al., "Strain monitoring of bismaleimide composites using embedded microcavity sensor," *Opt. Eng.* **55**(3), 037102 (2016).
14. S. E. Watkins, J. W. Fonda, and A. Nanni, "Assessment of an instrumented reinforced-concrete bridge with fiber-reinforced-polymer strengthening," *Opt. Eng.* **46**(5), 051010 (2007).
15. V. M. Murukeshan et al., "Cure monitoring of smart composites using fiber Bragg grating based embedded sensors," *Sens. Actuators A* **79**(2), 153–161 (2000).
16. N. J. Lawson et al., "Development and application of optical fibre strain and pressure sensors for in-flight measurements," *Meas. Sci. Technol.* **27**(10), 104001 (2016).
17. T. Yoshino et al., "Fiber-optic Fabry-Perot interferometer and its sensor applications," *IEEE Trans. Microwave Theory Tech.* **30**(10), 1612–1621 (1982).
18. M. R. Islam et al., "Chronology of Fabry–Perot interferometer fiber-optic sensors and their applications: a review," *Sensors* **14**(4), 7451–7488 (2014).
19. D. G. Lee et al., "Characterization of fiber optic sensors for structural health monitoring," *J. Compos. Mater.* **36**(11), 1349–1366 (2002).
20. G. Rajan et al., "Composite materials with embedded photonic crystal fiber interferometric sensors," *Sens. Actuators A* **182**, 57–67 (2012).
21. M. Ramakrishnan et al., "Hybrid fiber optic sensor system for measuring the strain, temperature, and thermal strain of composite materials," *IEEE Sens. J.* **14**(8), 2571–2578 (2014).
22. K. Yuksel et al., "Optical frequency domain reflectometry: a review," in *11th Int. Conf. Transparent Opt. Networks*, IEEE (2009).
23. J. Huang et al., "Spatially continuous distributed fiber optic sensing using optical carrier based microwave interferometry," *Opt. Express* **22**(15), 18757–18769 (2014).
24. Y. Du et al., "Distributed magnetic field sensor based on magnetostriction using Rayleigh backscattering spectra shift in optical frequency-domain reflectometry," *Appl. Phys. Express* **8**(1), 012401 (2014).
25. M. Froggatt and J. Moore, "High-spatial-resolution distributed strain measurement in optical fiber with Rayleigh scatter," *Appl. Opt.* **37**(10), 1735–1740 (1998).
26. X. Bao and L. Chen, "Recent progress in distributed fiber optic sensors," *Sensors* **12**(7), 8601–8639 (2012).
27. A. Minardo et al., "A reconstruction technique for long-range stimulated Brillouin scattering distributed fibre-optic sensors: experimental results," *Meas. Sci. Technol.* **16**(4), 900–908 (2005).
28. L. Wong et al., "Fatigue damage monitoring of a composite step lap joint using distributed optical fibre sensors," *Materials* **9**(5), 374 (2016).
29. R. Di Sante, "Fibre optic sensors for structural health monitoring of aircraft composite structures: recent advances and applications," *Sensors* **15**(8), 18666–18713 (2015).
30. G. P. Carman and G. P. Sendeckyj, "Review of the mechanics of embedded optical sensors," *J. Compos. Technol. Res.* **17**(3), 183–193 (1995).
31. P. Lesiak et al., "Influence of lamination process on optical fiber sensors embedded in composite material," *Measurement* **45**(9), 2275–2280 (2012).
32. M. Ramakrishnan et al., "The influence of thermal expansion of a composite material on embedded polarimetric sensors," *Smart Mater. Struct.* **20**(12), 125002 (2011).
33. Y. Du et al., "Rayleigh backscattering based macrobending single mode fiber for distributed refractive index sensing," *Sens. Actuators B* **248**, 346–350 (2017).
34. Y. Du et al., "Unclonable optical fiber identification based on Rayleigh backscattering signatures," *J. Lightwave Technol.* **35**(21), 4634–4640 (2017).
35. X. Gu, "Flat-cladding fiber Bragg grating sensors for large strain amplitude fatigue tests," in *Opto-Mechanical Fiber Optic Sensors*, H. Alemohammad, Ed., pp. 49–73, Butterworth-Heinemann, Oxford, United Kingdom (2018).
36. C. Y. Hong et al., "Measurement of cracks in concrete beams using a Brillouin optical time domain analysis sensing technology," in *Proc. Second Int. Postgrad. Conf. Infrastruct. and Environ. (supplement)*, Hong Kong (2010).
37. W. Challener et al., "Subsystem design and validation for optical sensors for monitoring enhanced geothermal systems," in *Proc. Thirty-Sixth Workshop Geotherm. Reservoir Eng.*, Vol. 31, Stanford University, Stanford, California (2011).
38. Z. Zhou, Z. Wang, and L. Shao, "Fiber-reinforced polymer-packaged optical fiber Bragg grating strain sensors for infrastructures under harsh environment," *J. Sens.* **2016**, 3953750 (2016).

Sasi Jothibasu is a graduate research assistant in the Lightwave Technology Laboratory of the Department of Electrical and Computer Engineering at Missouri University of Science and Technology.

Yang Du is a postdoc in the Lightwave Technology Laboratory of the Department of Electrical and Computer Engineering at Missouri University of Science and Technology.

Sudharshan Anandan is a graduate research assistant in the Department of Mechanical and Aerospace Engineering at Missouri University of Science and Engineering, Rolla, Missouri, USA.

Gurjot S. Dhaliwal is a graduate research assistant in the Department of Mechanical and Aerospace Engineering at Missouri University of Science and Engineering, Rolla, Missouri, USA.

Rex E. Gerald II is a visiting professor in the Lightwave Technology Laboratory of the Department of Electrical and Computer Engineering at Missouri University of Science and Technology (MS&T), has a BA degree in chemistry from the University of Chicago and a conjoint PhD from work conducted at the University of Illinois, Chicago and the Max Plank Institute, Heidelberg. He holds 25 US patents and more than 50 publications from research investigations at Argonne National Laboratory and MS&T.

Steve E. Watkins is a professor of electrical and computer engineering and director of the Applied Optics Laboratory at Missouri University of Science and Technology (formerly UM-Rolla), and has a PhD from the University of Texas at Austin. His memberships include SPIE (fellow member), IEEE (senior member), and ASEE. He was a distinguished visiting professor at the USAF Academy, an IEEE-USA congressional fellow, a visiting physicist at the Phillips Laboratory (USAF), and a visiting scholar at NTT (Japan).

K. Chandrashekhara is a professor in the Department of Mechanical and Aerospace Engineering at Missouri University of Science and Engineering, Rolla, Missouri, USA.

Jie Huang is a assistant professor of Electrical and Computer Engineering and director of the Lightwave Technology Laboratory at Missouri University of Science and Technology, and has a PhD in electrical engineering from Clemson University. His research interest mainly focuses on the development of optical and microwave micro/nano devices, sensors, and instrumentation for applications in energy, intelligent infrastructures, clean-environment, and biomedical systems.